An experimental and theoretical evaluation of the influence of pretargeting antibody on the tumor accumulation of effector

Guozheng Liu, Shuping Dou, Mary Rusckowski, and Donald J. Hnatowich

Division of Nuclear Medicine, Department of Radiology, University of Massachusetts Medical School, Worcester, Massachusetts

Abstract

In treating tumors by pretargeting, the antitumor antibody and the cytotoxic effector (e.g., toxins and radioactivity) are separately administered. Therefore, pretargeting is more complicated with many variables. We are conducting studies to understand the influence of each variable using a novel recognition pair of mutually complementary phosphorodiamidate morpholino oligomers (MORF/cMORF). Earlier we developed a semi-empirical model capable of accurately predicting the behavior of a radiolabeled cMORF effector with variations in dosages and timing. We have now extended the model to predict the effector behavior, in particular, its maximum percent tumor accumulation (MPTA) in mice pretargeted with three different MORF-conjugated antibodies (MN14, B72.3, and CC49). The MN14 and the CC49 target different antigens in the same tumor, whereas the CC49 and the B72.3 target the same antigen but with very different tumor accumulation. By comparing the pretargeting results of these three antibodies with our prediction, we confirmed that the MPTA of the radiolabeled cMORF effector in the LS174T tumor is independent of the antibodies. In conclusion, the MPTA cannot be improved through the use of different pretargeting antibodies, although different antibodies may improve the maximum absolute tumor accumulation, the heterogeneity, and/or the tumor-to-normal tissue ratios of the effector. This conclusion will apply equally well to effectors carrying a fluorescent probe, an anticancer agent, or a radioactive imaging agent. [Mol Cancer Ther 2008;7(5):1025–32]

Received 10/16/07; revised 1/23/08; accepted 1/27/08.

Grant support: NIH grants CA94994 and CA107360.

The costs of publication of this article were defrayed in part by the payment of page charges. This article must therefore be hereby marked *advertisement* in accordance with 18 U.S.C. Section 1734 solely to indicate this fact.

Requests for reprints: Guozheng Liu, Division of Nuclear Medicine, Department of Radiology, University of Massachusetts Medical School, 55 Lake Avenue North, Worcester, MA 01655-0243.
Phone: 508-856-1958; Fax: 508-856-4572.
E-mail: guozheng.liu@umassmed.edu

doi:10.1158/1535-7163.MCT-07-2203

Introduction

Pretargeting involves at least two injections, the first to target tumor with an antitumor antibody and the second to deliver the effector carrying a fluorescent probe, an anticancer agent, or an imaging radionuclide as in this study. Because this approach combines the superior tumor-targeting property of antibodies with the rapid pharmacokinetics of a small effector, it is proving to be increasingly useful for both tumor imaging and radiotherapy (1–5). It has been shown that pretargeting can greatly improve the tumor delivery of radionuclides over the conventional direct targeting by radiolabeled antibodies (6–11). Clinical radiotherapeutic trials are also showing promise in the treatment of solid tumors (12, 13). A novel pretargeting approach is under development in this laboratory using the recognition pair of an 18-mer phosphorodiamidate morpholino oligomer and its complement (MORF/cMORF; refs. 14, 15), as illustrated in Fig. 1.

For convenience, the pretargeting variables may be divided into two categories. For a two-step pretargeting approach, the variables of category 1 include tumor model, pretargeting antibody, and effector. The variables of category 2 include those relating to dosage and timing, specifically, the dosages of pretargeting antibody and effector, the pretargeting interval, and the detection time. We have developed a semi-empirical model to predict the biodistribution of the cMORF effector in pretargeted tumored mice with variations in the category 2 variables (16, 17). This prediction model is based on the pharmacokinetics of the pretargeting antibody, the pharmacokinetics of the radiolabeled effector administered alone, the accessibility of the antibody for the radiolabeled effector in the pretargeted tumor and normal tissues, the quantitative relationships between pretargeting antibody and effector, and finally the delivery property of the radiolabeled effector to the tumor and normal tissues. In this report, we are extending this model to investigate one category 1 variable, that is, the pretargeting antibody.

One important concept associated with the semi-empirical model and the category 1 variables is the maximum percent tumor accumulation (MPTA) of the cMORF effector in %ID or %ID/g. Our previous investigations indicated that, for a given solid tumor model (tumor host, type, size, and location) and a fixed dosage of pretargeting antibody, the absolute tumor accumulation of effector increases linearly with increasing effector dosage until saturation and then levels off (16, 17). When plotted as the percent accumulation (that is, %ID/g), the curve is horizontal until saturation and then declines. In the horizontal range, the percent accumulation corresponds to the MPTA. The MPTA and the constant slope of the

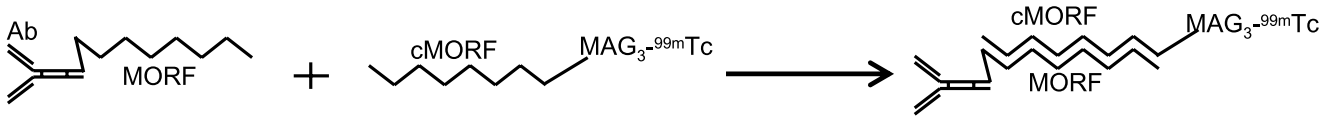

Figure 1. Principle of pretargeting using MORF oligomers as the recognition system.

absolute accumulation curve in the linear range are related by MPTA = slope × 100% / tumor weight. Similar dosage studies of effectors have been reported elsewhere although in less detail (18, 19).

It can be easily shown that the MPTA must be independent of the nature of pretargeting antibody. Recently (20), we have provided an expression of effector accumulation Q as a function of several factors:

$$Q\ (\%\mathrm{ID/g}) = F \times f \times W^{-1} \int_{t=0}^{t=\infty} E \times C(\%\mathrm{ID/g})_{\mathrm{blood}} \times dt$$

where F is the cardiac output (g/s), f is the fraction of the cardiac output reaching the tumor, W is the tumor weight (g), C is the blood level of the effector (%ID/g), and E is the trapping efficiency (the retained fraction of the effector reaching the tumor). If the dosage of cMORF effector is below that required to saturate the MORF antibody in tumor, E will be a constant. However, if the dosage of cMORF effector is above that required dosage, when the MORF in tumor becomes saturated, E will become zero such that the additional cMORF effector delivered to tumor cannot be retained. Thus, the percent tumor accumulation of cMORF effector just before the saturation of the pretargeting antibody in tumor will be the MPTA:

$$\mathrm{MPTA}\ (\%\mathrm{ID/g}) = F \times f \times W^{-1} \times E \int_{t=0}^{t=\infty} C(\%\mathrm{ID/g})_{\mathrm{blood}} \times dt \qquad (1)$$

This equation shows that the MPTA is independent of the pretargeting antibody and dependent only on the tumor and the effector. Thus, provided that the dosage does not exceed that dosage required to saturate the effector-binding sites presented by the pretargeting antibody in tumor, the percent tumor accumulation of the effector will be maximum at the value of MPTA and constant with increasing effector dosage. Of course, if the tumor model is changed, f may change and E may also be different due to the variance of diffusion barriers.

Prediction Model

Tumor. In this study, the experimental conditions were arranged to ensure that the tumor accumulation of the effector would be at MPTA. The effector dosage was selected based on the experimentally determined accessibility of the MORF–antibody for the labeled cMORF effector, the average number of MORF per antibody (gpm), and the MORF–antibody accumulation in tumor (%ID/g). We have shown that ^{111}In may be used to radiolabel the antibody MN14 for use in measuring its concentration in tumor and normal tissues and that ^{99m}Tc may be used to radiolabel the cMORF effector for use in measuring the accessibility of antibody in these tissues (16).

For an accessibility of 100% in tumor, the dosage of MORF– antibody (D_{antibody}; μg) that is required to be just saturated in tumor by any fixed effector dosage (D_{cMORF}; μg) can be calculated by Eq. (2):

$$D_{\mathrm{antibody}} = \frac{D_{\mathrm{cMORF}}}{M_{\mathrm{cMORF}}} \times \mathrm{MPTA} \times \frac{M_{\mathrm{antibody}}}{\%ID/g_{\mathrm{antibody}} \times \mathrm{gpm}} \qquad (2)$$

where $\%\mathrm{ID/g}_{\mathrm{antibody}}$ is the tumor accumulation of MORF–antibody and M_{antibody} and M_{cMORF} are the molecular weights of the antibody and cMORF effector, respectively.

Blood. By the nature of pretargeting, the radiolabeled effector is always designed to be excreted rapidly such that at the time of detection its blood level is usually minimal. In addition, at this time, the blood level of the pretargeting antibody will also be low and can be assumed to be a constant because of its slow pharmacokinetics. Thus, the total blood concentration of effector (C_{blood}) will be the sum of the concentrations of antibody-bound (bound C_{blood}) and free (free C_{blood}) effectors. The bound C_{blood} can be calculated from the saturation of the circulating antibody by Eq. (3), and as a first approximation, the free C_{blood} may be estimated from the experimental clearance curve of the labeled effector in tumored mice not receiving the pretargeting antibody (17). The accessibility of MORF antibody in blood has been shown to be ~100% (16).

$$\mathrm{Bound\ C_{blood}}(\%\mathrm{ID/g}) = \frac{D_{\mathrm{antibody}} \times \mathrm{Blood_{antibody}}(\%\mathrm{ID/g}) \times \mathrm{gpm} \times \mathrm{accessibility_{blood}}}{M_{\mathrm{antibody}}} \times \frac{M_{\mathrm{cMORF}}}{D_{\mathrm{cMORF}}} \qquad (3)$$

Normal Organs. In principle, the level in normal organs may be estimated in the same way as in blood. However, the following observation simplifies the estimation and eliminates the need to measure the accessibility. In our

previous studies with the MN14 antibody, over the wide range tested, we found that the organ-to-blood ratios of antibody-bound effector are constant in all organs other than kidneys (see immediately below), independent of the dosages of antibody and effector as well as the pretargeting interval. Our interpretation is that the accessible MORF-MN14 in these normal organs is in equilibrium with MORF-MN14 in blood (17). As described below, we show that this equilibrium of MORF–antibodies between normal organs and blood still holds for MORF-CC49 and MORF-B72.3 as well.

Kidney. The kidney is a unique organ with respect to pretargeting because the cMORF effector clears exclusively via this organ and its accumulation is independent of the presence or absence of MORF–antibody therein (17). Thus, the kidney accumulation is a property of the radiolabeled cMORF effector and independent of the pretargeting antibody provided that any pharmacokinetic effects can be ignored. For example, if the blood level of a particular antibody is unusually high at the time of effector administration, more of the effector will be bound in circulation and less will be free to clear and accumulate in the kidneys. However, this high level of antibody is seldom encountered in pretargeting.

Based on the above semi-empirical model and the MPTA expression, we now report on the agreement of the experimental results with predictions in pretargeting with three different antibodies. The anti-CEA antibody MN14 and the anti-TAG-72 antibody CC49 target different antigens in the same tumor, whereas the CC49 and B72.3 target the same TAG-72 antigens but with a large difference in tumor accumulation.

Materials and Methods

As before, the base sequences of MORF and its complement (cMORF) were 5′-TCTTCTACTTCACAACTA-linker-amine and 5′-TAGTTGTGAAGTAGAAGA-linker-amine (GeneTools), respectively. The murine anti-CEA antibody MN14 was a gift from Immunomedics. The anti-TAG-72 antibody CC49, also murine, was produced by Strategic Biosolutions from the CC49 murine hybridoma cell line, a gift from Dr. Schlom (Laboratory of Tumor Immunology and Biology, Center for Cancer Research, National Cancer Institute, NIH). The first-generation anti-TAG-72 antibody B72.3 was a gift from National Cancer Institute Biometric Research Branch Preclinical Repository. The *S*-acetyl NHS-MAG_3 was synthesized in-house (21) and the structure was confirmed by elemental analysis, proton nuclear magnetic resonance, and mass spectroscopy. The Hydralink linker was from Solulink Biosciences. The DTPA cyclic anhydride was from Sigma. The *p*-SCN-Benzyl-DTPA was from Macrocyclics. The P-4 resin (Bio-Gel P-4 Gel, medium) was purchased from Bio-Rad Laboratories and the Sephadex G-100 resin was from Pharmacia Biotech. The ^{99}Mo-^{99m}Tc generator and the $^{111}InCl_3$ were both from Perkin-Elmer Life Science. All other chemicals were reagent grade and used without purification.

^{99m}Tc-Labeled cMORF, ^{111}In-Labeled Antibodies, and MORF-Conjugated Antibodies

The MAG_3-cMORF was synthesized as described previously (22). To radiolabel, 50 μL ^{99m}Tc-pertechnetate generator eluate was introduced into a combined solution consisting of 30 μL (>0.5 μg) of MAG_3-MORF in NH_4OAc buffer (pH 5.2), 10 μL of 50 μg/μL Na_2 tartrate·$2H_2O$ in a pH 9.2 buffer, and 3 μL of 4 μg/μL $SnCl_2$·$2H_2O$ in ascorbate-HCl solution (1 μg/μL sodium ascorbate in 10 mmol/L HCl). The solution was heated at 100°C for 20 min. The labeling efficiency was routinely >95% as determined by size-exclusion high-performance liquid chromatography.

Although the MN14 and B72.3 were successfully conjugated with the DTPA cyclic anhydride as described previously (15), difficulties were experienced in conjugating the CC49 and labeling with ^{111}In in this manner. Therefore, *p*-SCN-benzyl-DTPA was used for this antibody. Briefly, a CC49 solution (1.7 μg/μL) in 20 mmol/L PBS (pH 7.2) was mixed with a 0.80 μg/μL *p*-SCN-benzyl-DTPA solution in 0.5 mol/L $NaCO_3$-$NaHCO_3$ buffer (molar ratio = 2/8; pH 9.3) at a DTPA-to-antibody molar ratio of 55 and the mixture allowed to react overnight (15-24 h). The average number of DTPA per antibody (gpm) was determined by analyzing the ^{111}In-labeled conjugation mixture by size-exclusion high-performance liquid chromatography before purification and was calculated by multiplying the DTPA-to-antibody molar ratio by the fraction of radioactivity on the antibody. Purification was achieved on a 0.7 × 20 cm Sephadex G-100 glass Econo-column. The labeling with ^{111}In of the three antibodies was as described previously (15).

The MORF–antibodies were synthesized using a commercial Hydralink linker (23). The antibodies were first conjugated with succinimidyl 4-hydrazinonicotinate acetone hydrazone, whereas the MORF was conjugated with succinimidyl 4-formylbenzoate. After purification, combining the hydrazine-modified antibody and the benzaldehyde-modified MORF resulted in hydrazone formation. Purification of the MORF–antibodies from the free MORF was also achieved on a 0.7 × 20 cm Sephadex G-100 glass Econo-column and the gpm was determined following routine procedure described previously (15).

Animal Study

All animal studies were done with the approval of the University of Massachusetts Medical School Institutional Animal Care and Use Committee. For tumor induction, 10^6 LS174T colon cancer cells were injected into the left thigh of each Swiss NIH nude mouse (Taconic Farms). The animals were used at 12 to 13 days when the tumors were ~0.5 g. To measure the biodistribution of each antibody, three groups (n = 4) of tumored mice received via a tail vein 30 μg (20-30 μCi) ^{111}In-labeled B72.3, MN14, or CC49. After 48 h, the mice were sacrificed for biodistribution by exsanguination via heart puncture under halothane anesthesia. In the pretargeting studies, three groups (n = 4) of tumored mice received via a tail vein 48, 23, and 11 μg MORF-conjugated B72.3, MN14, and CC49, respectively.

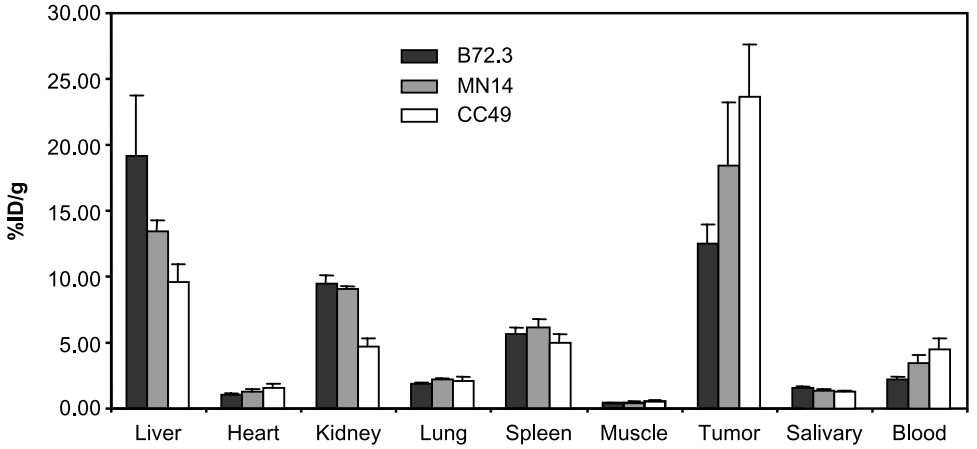

Figure 2. Biodistributions (%ID/g) of the three ^{111}In-labeled antibodies at 48 h. Bars, 1 SD (n = 4).

After 48 h, each mouse received 1 μg (100 μCi) labeled cMORF also via a tail vein. Animals were sacrificed for biodistribution 3 h later.

At sacrifice, samples of blood and other organs were removed, weighed, and counted in a NaI(Tl) well counter (Cobra II automatic gamma counter; Packard Instrument) along with a standard of the injectate. Blood and muscle were assumed to constitute 7% and 40% of body weight, respectively. The tumored thigh was excised and the skin and as much of the muscle and bone as possible were removed before counting. The radioactivity therein was attributed to the tumor because the radioactivity levels in bone and muscle were negligible. After the tumor thigh was counted, the tumor mass was dissected to isolate the residual bone and muscle so that their weights could be subtracted to provide the net tumor weight.

Results

Biodistribution of ^{111}In-Labeled Antibodies

The 48-h biodistributions of the three antibodies radiolabeled with ^{111}In in LS174T tumored mice are presented in Fig. 2. As shown, whereas the accumulations in heart, lung, spleen, muscle, and salivary gland were generally antibody independent, the liver accumulations were highly dependent. Significant differences in kidney accumulations occurred only for the labeled CC49 antibody (Student's t test, $P < 0.05$). The tumor accumulations varied in proportion to the blood levels such that the tumor-to-blood ratios for these antibodies are essentially identical (5.6, 5.4, and 5.3 for B72.3, MN14, and CC49, respectively). The 48-h tumor accumulations of the ^{111}In-labeled antibodies in %ID/g and corresponding average tumor weights (in parentheses) were 12.5 ± 1.4 (0.65 ± 0.12 g), 16.7 ± 3.9 (0.58 ± 0.13 g), and 23.6 ± 4.0 (0.57 ± 0.13 g) for B72.3, MN14, and CC49, respectively.

Biodistribution of Labeled cMORF in Pretargeted Mice

The conjugation of B72.3, MN14, and CC49 with MORF provided an average of 0.53, 0.83, and 1.22 gpm, respectively. The tumor accumulation of the cMORF effector earlier determined in the mice pretargeted with MORF-MN14, 6.24 ± 0.41%ID/g for a 0.52 ± 0.05 g LS174T tumor, was predicted to be the MPTA of cMORF effector in this study with each of the three antibodies (17). Using the molecular weights of cMORF (6331 Da) and antibody (160 kDa) and the 48-h ^{111}In-antibody tumor accumulations (Fig. 2), the dosage of MORF–antibody that must be administered such that the accessible MORFs in tumor at 48 h are just saturated with the cMORF effector can be estimated by Eq. (2) for any given dosage of cMORF effector. In this manner and assuming the MPTA is independent of antibody, the calculation for an effector dosage of 2 μg provides 48, 23, and 11 μg as the dosages of MORF conjugated B72.3, MN14, and CC49, respectively. When these antibody dosages were used in the animal studies, the dosage of effector was reduced from 2 to 1 μg to ensure the MORF binding sites in tumor would not be saturated (that is, MPTA conditions).

Table 1 lists the 3-h biodistributions of labeled cMORF effector in tumored mice pretargeted 48 h earlier by each of the three MORF–antibodies at the dosages selected. Because the labeled cMORF effector was administered at a dosage lower than that required for saturation, the tumor

Table 1. 3-h biodistributions (%ID/g) of labeled cMORF effector in tumored mice pretargeted 48 h earlier by one of the MORF-MN14, MORF-CC49, and MORF-B72.3 antibodies

Organ	MN14	CC49	B72.3
Liver	0.84 ± 0.15	0.63 ± 0.08	1.35 ± 0.24
Heart	0.55 ± 0.09	0.30 ± 0.05	0.85 ± 0.24
Kidney	4.10 ± 1.33	3.57 ± 0.71	3.41 ± 0.48
Lung	0.85 ± 0.16	0.68 ± 0.06	1.38 ± 0.41
Spleen	0.44 ± 0.06	0.41 ± 0.05	0.77 ± 0.15
Muscle	0.33 ± 0.19	0.18 ± 0.03	0.45 ± 0.13
Tumor	6.28 ± 1.47	6.16 ± 0.47	8.89 ± 1.28
Salivary gland	0.59 ± 0.11	0.44 ± 0.07	1.02 ± 0.24
Blood	2.26 ± 0.38	1.60 ± 0.09	3.75 ± 0.99
Tumor size (g)	0.50 ± 0.09	0.54 ± 0.11	0.43 ± 0.23

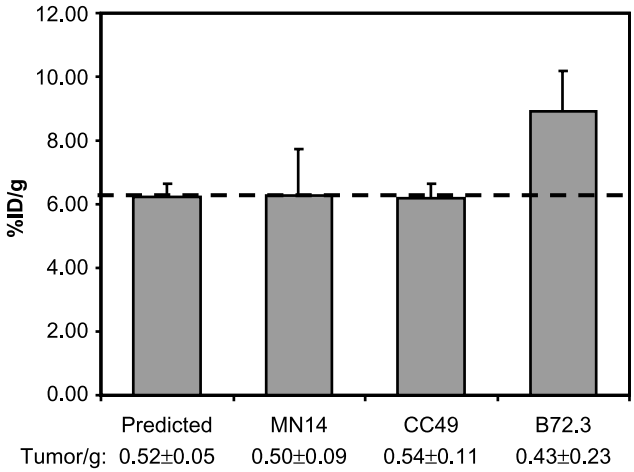

Figure 3. Tumor accumulations of effector at 3 h by pretargeting with three different MORF–antibodies 48 h earlier. Bars, 1 SD (n = 4). The *horizontal line* at 6.24%ID/g is the predicted value.

accumulations should be the MPTAs. The experimental values in each organ are now compared with the theoretical expectations below.

Tumor. Because both the pharmacokinetics and the average number of MORF per antibody differed among the antibodies, the dosage of each MORF–antibody was adjusted to provide the same accessible MORF concentration in tumor. Otherwise, a different dosage of effector would be required to meet the MPTA conditions for each antibody.

Figure 3 shows the experimental MPTAs from Table 1 along with the corresponding average tumor size (g). The tumor accumulations (6.28 ± 1.47 and 6.16 ± 0.47 %ID/g) at 3 h in mice pretargeted 48 h earlier with the MORF-MN14 and MORF-CC49 antibodies are statistically identical to each other and to that predicted (6.24 ± 0.41%ID/g), whereas that for MORF-B72.3 (8.89 ± 1.28%ID/g) is significantly higher than predicted (Student's t test, $P < 0.05$). We have observed previously an inverse relationship between tumor accumulation and tumor size (17) to suggest that the higher tumor accumulation in this case is most likely due to the smaller tumor size of 0.43 g.

Blood. At the detection time of 3 h, the blood level of free effector was earlier determined to be 0.04%ID/g (15). The total blood levels of effector can then be predicted by adding this free effector level to the antibody-bound effector levels calculated from Eq. (3). In animals pretargeted 48 h earlier with the MORF-MN14, the experimental blood level of cMORF effector agrees well within 2 SDs with the predicted as shown in Table 2A; 1 SD was fixed at 25% of the predicted as before (17). The difference in the case of animals receiving MORF-B72.3 is just outside this limit, whereas the difference in the case of MORF-CC49 is larger. These discrepancies may be related to different pharmacokinetic behavior of the ^{111}In-DTPA-antibody used to trace the pharmacokinetics of the MORF-conjugated antibody.

Liver, Spleen, Lung, Heart, and Muscle. As mentioned above, the organ-to-blood ratios of antibody-bound effector were earlier found experimentally to be constants with respect to the dosages of antibody and effector as well as the pretargeting interval (17). The experimental and predicted ratios from this study are listed in Table 2B. To derive these experimental ratios, it was necessary to obtain the value for the bound effector by subtracting the free effector level in each normal organ from the experimental organ accumulations in the same manner as that described above for blood. The free effector levels at 3 h were earlier determined to be 0.27, 0.17, 0.12, 0.06, and 0.03 %ID/g for liver, spleen, lung, heart, and muscle, respectively (17). As shown, the experimental ratios for all three antibodies are within 2 SDs of that predicted. The predicted ratios in the table are taken from previous pretargeting studies with MN14 (17) and reproduced in this study. As is evident in Table 2B, the ratios for the pretargeting using B72.3 and CC49 antibodies are also in agreement with the predicted.

Kidney. The kidney accumulations of the effector were 3.41 ± 0.48, 4.10 ± 1.33, and 3.57 ± 0.71 %ID/g (Table 1) in the mice pretargeted with MORF-conjugated B72.3, MN14, and CC49, respectively, and agree within 2 SDs with the predicted 5.44 ± 1.51%ID/g obtained from the kidney accumulations measured during several previous studies (17), again reflecting that the kidney accumulation is a determinant of the effector only. In our case, the influence of the different pharmacokinetics of each antibody on the kidney levels of MORF may be neglected because, independent of the antibody, most of the effector clears through the kidneys at 3 h (15).

Table 2. Comparisons between experimental and predicted values for blood levels (%ID/g) and organ-to-blood ratios of antibody-bound effector at 3 h postinjection of cMORF effector in LS174T tumored mice having received one of three MORF-conjugated antibodies 48 h before injection of cMORF effector

(A) Blood level

	B72.3	MN14	CC49
Experimental	3.75 ± 0.99	2.26 ± 0.38	1.60 ± 0.09
Predicted	2.27 ± 0.57	2.51 ± 0.63	2.41 ± 0.60

(B) Organ-to-blood ratios

	Predicted*	B72.3	MN14	CC49
Liver/blood	0.31	0.30 ± 0.08	0.26 ± 0.03	0.23 ± 0.05
Spleen/blood	0.15	0.16 ± 0.02	0.12 ± 0.02	0.15 ± 0.04
Lung/blood	0.40	0.34 ± 0.06	0.33 ± 0.05	0.36 ± 0.04
Heart/blood	0.20	0.21 ± 0.01	0.22 ± 0.00	0.15 ± 0.03
Muscle/blood	0.11	0.11 ± 0.02	0.14 ± 0.09	0.10 ± 0.02

NOTE: Values presented as the average with 1 SD (n = 4).
*Taken from (17).

Discussion

We showed previously that the biodistribution of the cMORF effector in pretargeted mice can be predicted by our semi-empirical model with variations in three category 2 variables, that is, the dosage of pretargeting antibody, the dosage of effector, and the pretargeting interval (17). Therefore, this approach may help avoid trial-and-error studies of pretargeting optimization. Several rules govern the selection of the category 2 variables for optimal pretargeting. The pretargeting interval should be selected to provide the required tumor-to-blood ratio. The detection time should be selected to allow the free effector to clear to the background radioactivity level required. The dosage of the pretargeting antibody is not a critical variable because any convenient dosage may be selected, although it should be below that required to saturate the tumor antigenic sites. With a too high antibody dosage, higher than necessary levels of antibody will be present in circulation and normal organs at the time of effector administration. To achieve an optimal pretargeting outcome, the effector dosage should be such that the accessible antibody localized in tumor is just saturated by the effector. A lower effector dosage will still provide the MPTA (%ID or %ID/g) but a lower absolute accumulation (in nmol or ng), thus providing a less favorable tumor-to-blood ratio. Conversely, an effector dosage in excess of that necessary to saturate the antibody in tumor will still provide the maximum absolute accumulation but a lower percent tumor accumulation, because a less percent of the effector will be retained in tumor.

In this study, we have extended the semi-empirical model to predict the influence of the category 1 variables, although the utility of our model regarding these variables is still qualitative. At this stage, all the variables in the MPTA expression of Eq. (1) are not available. However, some predictions from this expression may improve our understanding of tumor delivery. In particular, we have predicted that the MPTA is independent of antibody based on Eq. (1), whether targeting different antigens or having different pharmacokinetics. This experimental study has confirmed this prediction. Recently, we had also shown that the gpm of an antibody does not change the MPTA (23).

In the course of our investigations, several misconceptions residing in this and possibly other laboratories have become clarified. Firstly, for solid tumors, the MPTA of the effector cannot be increased by increasing the number of effector-binding sites in tumor, for example, by administering a larger dosage of antibody (17), by increasing the gpm (23), or by other means (however, it is possible to increase the absolute tumor accumulation by, for example, amplification pretargeting, in which a multivalent polymer is administered between the pretargeting antibody and the effector; ref. 24). Secondly, the benefit of pretargeting is usually not in achieving a higher absolute or percent tumor accumulation compared with conventional targeting, because the rapid clearance of the effector limits its delivery; therefore, the absolute or percent tumor accumulations by pretargeting is often lower than that achievable by conventional targeting. Thirdly, pretargeting cannot provide tumor-to-blood ratios superior to that achieved by directly labeled antibody because the effector cannot target more pretargeted antibody than exists in tumor and normal tissues. However, as mentioned earlier, the advantage of pretargeting rests in combining the tumor affinity of the antitumor antibody with the rapid clearance of the effector (6–11). In this way, pretargeting can greatly improve the tumor delivery of cytotoxic agents, such as radioactive effectors, by providing a comparable tumor-to-blood ratio in ~1 h postadministration of the effector to that achieved by radiolabeled antibodies in days and therefore greatly reduce the cytotoxicity to normal tissues.

However, it should be mentioned that certain tumor-to-normal-organ ratios may increase if the antibody in those organs, but not in tumor, become inaccessible to the effector due to metabolism or some other mechanism (25–27). In our experience, this phenomenon applies especially to liver in the case of MORF pretargeting. For example, in this investigation, the liver accumulations of CC49, MN14, and B72.3 measured by the ^{111}In-labeled antibodies were 9.6, 13.4, and 19.2 %ID/g, respectively, at 48 h (Fig. 2). If the accessibility of the MORF–antibodies for the cMORF effector were 100%, the liver accumulations would have been ~5.1, 10.1, and 19.3 %ID/g based on Eq. (3) rather than the much lower observed accumulations of 0.63, 0.84, and 1.35 %ID/g (Table 1).

To our knowledge, this report describes the first comparison of different antibodies for pretargeting under MPTA conditions. Several previous studies have compared different antibodies for pretargeting and reported antibody-dependent differences in the tumor accumulation of effector (8, 28–31). However, these earlier studies compared antibodies at the same dosage of antibodies and the same dosage of effector without considering the saturation of pretargeting antibody by effector in tumor. In this investigation, if each of the three antibodies had been administered at the same dosage and the effector were at a fixed dosage sufficient to saturate any of the three MORF–antibodies in tumor, the CC49 would have similarly provided a higher tumor accumulation of the effector than the other two. However, even in the case of CC49, the effector accumulation would have been lower than that achieved herein under the MPTA conditions.

Although the MPTA cannot be improved by the use of different antibodies, there is often a need to consider different antibodies for pretargeting (32). Advanced recombinant and antibody engineering technologies are now increasingly in use to develop antitumor antibodies with improved specificity, diminished cross-reactivity with normal tissues, increased binding affinity, alleviated immunogenicity, reduced heterogeneity of antibody deposition in tumor, etc. These include intact antibodies targeting different antigens, antibodies with different pharmacokinetics, antibody fragments, and genetically engineered small antibody constructs (diabodies, minibodies, affibodies, etc.). Reports on a large number of these pretargeting studies have appeared in recent years (33–36). Furthermore, if the dosage of effector is above that required

to saturate the MORF–antibody in tumor, both the absolute and the percent tumor accumulation of the effector will depend on the antibody, because antibodies differ in tumor accumulation (28), affinity for their antigen or the effector (37), the disappearance rate by either internalization or shedding of their antigen complexes, and the accessibility in tumor for the effector (38, 39).

In conclusion, from the results in mice pretargeted with three different antibodies, we have confirmed experimentally the prediction that the MPTA of the effector is independent of the pretargeting antibody in the LS174T tumor model. Although it is possible to improve tumor-to-normal-tissue ratios, the use of different antibodies cannot improve the MPTA of labeled cMORF effector by pretargeting. Although this investigation is concerned with an effector radiolabeled with an imaging radionuclide, the conclusions arrived at herein will apply equally well to effectors carrying other imaging labels such as fluorophores or cytotoxic labels such as therapeutic radionuclides.

Disclosure of Potential Conflicts of Interest

No potential conflicts of interest were disclosed.

Acknowledgments

We thank Dr. Griffiths (Immunomedics) for providing the anti-CEA antibody MN14, Dr. Schlom for providing the CC49 hybridoma, and Dr. Raurgemma (National Cancer Institute Biometric Research Branch Preclinical Repository) for providing the B72.3 antibody.

References

1. Sharkey RM, Goldenberg DM. Advances in radioimmunotherapy in the age of molecular engineering and pretargeting. Cancer Invest 2006;24:82–97.

2. Reilly RM. Radioimmunotherapy of solid tumors: the promise of pretargeting strategies using bispecific antibodies and radiolabeled haptens. J Nucl Med 2006;47:196–9.

3. Goldenberg DM, Sharkey RM, Paganelli G, Barbet J, Chatal JF. Antibody pretargeting advances cancer radioimmunodetection and radioimmunotherapy. J Clin Oncol 2006;24:823–34.

4. Corneillie TM, Whetstone PA, Meares CF. Irreversibly binding antimetal chelate antibodies: artificial receptors for pretargeting. J Inorg Biochem 2006;100:882–90.

5. Sharkey RM, Karacay H, Cardillo TM, et al. Improving the delivery of radionuclides for imaging and therapy of cancer using pretargeting methods. Clin Cancer Res 2005;11:7109–21s.

6. Karacay H, Brard PY, Sharkey RM, et al. Therapeutic advantage of pretargeted radioimmunotherapy using a recombinant bispecific antibody in a human colon cancer xenograft. Clin Cancer Res 2005;11:7879–85.

7. Sharkey RM, Cardillo TM, Rossi EA, et al. Signal amplification in molecular imaging by pretargeting a multivalent, bispecific antibody. Nat Med 2005;11:1250–5.

8. Pagel JM, Hedin N, Subbiah K, et al. Comparison of anti-CD20 and anti-CD45 antibodies for conventional and pretargeted radioimmunotherapy of B-cell lymphomas. Blood 2003;101:2340–8.

9. Subbiah K, Hamlin DK, Pagel JM, et al. Comparison of immunoscintigraphy, efficacy, and toxicity of conventional and pretargeted radioimmunotherapy in CD20-expressing human lymphoma xenografts. J Nucl Med 2003;44:437–45.

10. Magnani P, Paganelli G, Modorati G, et al. Quantitative comparison of direct antibody labeling and tumor pretargeting in uveal melanoma. J Nucl Med 1996;37:967–71.

11. Sung C, van Osdol WW. Pharmacokinetic comparison of direct antibody targeting with pretargeting protocols based on streptavidin-biotin binding. J Nucl Med 1995;36:867–76.

12. Kraeber-Bodéré F, Rousseau C, Bodet-Milin C, et al. Targeting, toxicity, and efficacy of 2-step, pretargeted radioimmunotherapy using a chimeric bispecific antibody and ^{131}I-labeled bivalent hapten in a phase I optimization clinical trial. J Nucl Med 2006;47:247–55.

13. Forero-Torres A, Shen S, Breitz H, et al. Pretargeted radioimmunotherapy (RIT) with a novel anti-TAG-72 fusion protein. Cancer Biother Radiopharm 2005;20:379–90.

14. Liu G, Mang'era K, Liu N, Gupta S, Rusckowski M, Hnatowich DJ. Tumor pretargeting in mice using ^{99m}Tc-labeled morpholino, a DNA analog. J Nucl Med 2002;43:384–91.

15. Liu G, He J, Dou S, et al. Pretargeting in tumored mice with radiolabeled morpholino oligomer showing low kidney uptake. Eur J Nucl Med Mol Imaging 2004;31:417–24.

16. Liu G, He J, Dou S, Gupta S, Rusckowski M, Hnatowich DJ. Further investigations of morpholino pretargeting in mice—establishing quantitative relations in tumor. Eur J Nucl Med Mol Imaging 2005;32:1115–23.

17. Liu G, Dou S, He J, Liu X, Rusckowski M, Hnatowich. Predicting the biodistribution of radiolabeled cMORF effector in MORF-pretargeted mice. Eur J Nucl Med Mol Imaging 2007;34:237–46.

18. Sharkey RM, Karacay H, Richel H, et al. Optimizing bispecific antibody pretargeting for use in radioimmunotherapy. Clin Cancer Res 2003;9:3897–913S.

19. Gautherot E, Le Doussal JM, Bouhou J, et al. Delivery of therapeutic doses of radioiodine using bispecific antibody-targeted bivalent haptens. J Nucl Med 1998;39:1937–43.

20. Liu G, Dou S, Pretorius PH, Liu X, Rusckowski M, Hnatowich DJ. Pretargeting CWR22 prostate tumor in mice with MORF-B72.3 antibody and radiolabeled cMORF. Eur J Nucl Med Mol Imaging. Epub 2007. PMID:17909792.

21. Winnard P, Jr., Chang F, Rusckowski M, Mardirossian G, Hnatowich DJ. Preparation and use of NHS-MAG3 for technetium-99m labeling of DNA. Nucl Med Biol 1997;24:425–32.

22. Liu G, Dou S, He J, et al. Radiolabeling of MAG_3-morpholino oligomers with ^{188}Re at high labeling efficiency and specific radioactivity for tumor pretargeting. Appl Radiat Isot 2006;64:971–8.

23. He J, Liu G, Dou S, Gupta S, Rusckowski M, Hnatowich DJ. An improved method for covalently conjugating morpholino oligomers to antitumor antibodies. Bioconjug Chem 2007;18:983–8.

24. He J, Liu G, Gupta S, Zhang Y, Rusckowski M, Hnatowich DJ. Amplification targeting: a modified pretargeting approach with potential for signal amplification-proof of a concept. J Nucl Med 2004;45:1087–95.

25. Liu G, Liu C, Zhang S, et al. Investigations of ^{99m}Tc morpholino pretargeting in mice. Nucl Med Commun 2003;24:697–705.

26. Goodwin DA, Meares CF, Watanabe N, et al. Pharmacokinetics of pretargeted monoclonal antibody 2D12.5 and ^{88}Y-Janus-2-(*p*-nitrobenzyl)-1,4,7,10-tetraazacyclododecanetetraacetic acid (DOTA) in BALB/c mice with KHJJ mouse adenocarcinoma: a model for 90Y radioimmunotherapy. Cancer Res 1994;54:5937–46.

27. Liu G, Zhang S, He J, et al. The influence of chain length and base sequence on the pharmacokinetic behavior of ^{99m}Tc-morpholinos in mice. Q J Nucl Med 2002;46:233–43.

28. Karacay H, Sharkey RM, McBride WJ, et al. Pretargeting for cancer radioimmunotherapy with bispecific antibodies: role of the bispecific antibody's valency for the tumor target antigen. Bioconjug Chem 2002;13:1054–70.

29. Cardillo TM, Karacay H, Goldenberg DM, et al. Improved targeting of pancreatic cancer: experimental studies of a new bispecific antibody, pretargeting enhancement system for immunoscintigraphy. Clin Cancer Res 2004;10:3552–61.

30. Rossi EA, Sharkey RM, McBride W, et al. Development of new multivalent-bispecific agents for pretargeting tumor localization and therapy. Clin Cancer Res 2003;9:3886–96S.

31. van Schaijk FG, Boerman OC, Soede AC, et al. Comparison of IgG and F(ab)2 fragments of bispecific anti-RCCxanti-DTIn-1 antibody for pretargeting purposes. Eur J Nucl Med Mol Imaging 2005;32:1089–95.

32. Goldenberg DM, Sharkey RM, Barbet J, Chatal J-F. Radioactive antibodies: selective targeting and treatment of cancer and other diseases. Appl Radiol 2007;36:10–29.

33. Rossi EA, Goldenberg DM, Cardillo TM, McBride WJ, Sharkey RM, Chang CH. Stably tethered multifunctional structures of defined composition made by the dock and lock method for use in cancer targeting. Proc Natl Acad Sci U S A 2006;103:6841 – 6.

34. Albrecht H, Denardo GL, Denardo SJ. Monospecific bivalent scFv-SH: effects of linker length and location of an engineered cysteine on production, antigen binding activity and free SH accessibility. J Immunol Methods 2006;310:100 – 16.

35. Nobs L, Buchegger F, Gurny R, Allemann E. Biodegradable nanoparticles for direct or two-step tumor immunotargeting. Bioconjug Chem 2006;17:139 – 45.

36. Zhang S, Xing J, Zhang Q, et al. Optimal design of Ig 5′ primers for construction of diverse phage antibody library established to select anti-HAb18GEF and anti-DOTA-Y Fabs for hepatoma pretargeting RIT. Front Biosci 2006;11:1733 – 49.

37. Barbet J, Kraeber-Bodere F, Vuillez JP, Gautherot E, Rouvier E, Chatal JF. Pretargeting with the affinity enhancement system for radioimmunotherapy. Cancer Biother Radiopharm 1999;14:153 – 66.

38. Casalini P, Luison E, Menard S, Colnaghi MI, Paganelli G, Canevari S. Tumor pretargeting: role of avidin/streptavidin on monoclonal antibody internalization. J Nucl Med 1997;38:1378 – 81.

39. Muzykantov VR, Christofidou-Solomidou M, Balyasnikova I, et al. Streptavidin facilitates internalization and pulmonary targeting of an anti-endothelial cell antibody (platelet-endothelial cell adhesion molecule 1): a strategy for vascular immunotargeting of drugs. Proc Natl Acad Sci U S A 1999;96:2379 – 84.

Molecular Cancer Therapeutics

An experimental and theoretical evaluation of the influence of pretargeting antibody on the tumor accumulation of effector

Guozheng Liu, Shuping Dou, Mary Rusckowski, et al.

Mol Cancer Ther 2008;7:1025-1032.